

Recreating Fundamental Effects in the Laboratory?

Ralf Schützhold*

Fachbereich Physik, Universität Duisburg-Essen, D-47048 Duisburg, Germany

This article provides a brief (non-exhaustive) overview of some possibilities for recreating fundamental effects which are relevant for black holes (and other gravitational scenarios) in the laboratory. Via suitable condensed matter analogues and other laboratory systems, it might be possible to model the Penrose process (superradiant scattering), the Unruh effect, Hawking radiation, the Eardley instability, black-hole lasers, cosmological particle creation, the Gibbons-Hawking effect, and the Schwinger mechanism. Apart from an experimental verification of these yet unobserved phenomena, the study of these laboratory systems might shed light onto the underlying ideas and problems and should therefore be interesting from a (quantum) gravity point of view as well.

Keywords: Penrose process (superradiant scattering), Unruh effect, Hawking radiation, Eardley instability, black-hole laser, cosmological particle creation, Gibbons-Hawking effect, Schwinger mechanism, analogue gravity

I. INTRODUCTION

Under the influence of extreme conditions, such as the strong gravitational field around black holes, matter – and even the vacuum – behaves in unexpected ways and shows many fascinating phenomena¹ like Hawking radiation². Although extremely hard to observe, these striking effects are very interesting from a fundamental point of view for our understanding of black holes and (quantum) gravity. For example, Hawking's discovery of black hole evaporation² surprisingly confirmed Bekenstein's thermodynamic interpretation³ of black holes. Understanding this link to thermodynamics including the origin of the black hole entropy and the related black hole information “paradox” is one of the key questions of quantum gravity.

Since the options for an experimental or observational approach to these problems are rather limited, an alternative possibility would be to recreate the aforementioned phenomena in suitable laboratory settings^{4–8}. This idea will be pursued in the following. After a short review of the fundamental effects under consideration in Sec. II, the underlying idea of analogue gravity is presented in Sec. III. In Sec. IV, these ideas are then applied to several laboratory systems which may allow us to recreate the fundamental effects discussed in Sec. II. Finally, Sec. V is devoted to the question of what can be learnt from studying these analogies and the outline of future directions.

II. FUNDAMENTAL EFFECTS

Let us start with a brief review of the fundamental effects under consideration together with some of their relevant features. Familiarity of the reader with the basic

concepts of general relativity and quantum field theory is assumed – even though the main points should (hopefully) also become evident to all other readers.

A. Penrose Process – Superradiance

In a stationary (i.e., time-independent) metric, it is possible to derive a locally conserved energy density for the matter fields – as expected from the Noether theorem. (Otherwise, i.e., in a genuinely time-dependent metric, there will be an exchange of energy between the gravitational field and the matter fields in general.) For example, the conserved energy density of a massless (and minimally coupled) scalar field reads ($\hbar = c = G_N = k_B = 1$)

$$T_0^0 = \frac{1}{2} g^{00} \dot{\Phi}^2 - \frac{1}{2} g^{ij} (\partial_i \Phi) (\partial_j \Phi). \quad (1)$$

Let us specify the second part for the equatorial plane of the Kerr metric⁹ describing a rotating black hole

$$g^{\varphi\varphi} \left(\vartheta = \frac{\pi}{2} \right) = -\frac{1 - \frac{2M}{r}}{\Delta}, \quad (2)$$

with $\Delta = r^2 - 2Mr + a^2$, where M is the (ADM) mass of the black hole and a measures its rotation. The inner and outer horizons occur at $r_{\pm} = M \pm \sqrt{M^2 - a^2}$, i.e., where $\Delta = 0$. However, even outside the horizons, there is a region where $g^{\varphi\varphi}$ becomes negative, which is called the ergo-region $r_{\text{ergo}}(\vartheta = \pi/2) = 2M > r_{\pm}$. Remembering Eq. (1), we see that the conserved energy density may become negative in this region. This fascinating observation motivates the following striking phenomenon: Imagine a wave-packet stemming from spatial infinity (i.e., with a positive energy) which propagates into the ergo-region and splits up inside this region into a wave-packet which escapes to infinity and another part which crosses the (outer) horizon and is then trapped by the black hole. Now, if the second (trapped) part has a negative energy – which is possible inside the ergo-sphere – the remaining

*Electronic address: ralf.schuetzhold@uni-due.de

part which escapes to infinity must have an energy which is greater than that of the incoming wave-packet due to energy conservation! Replacing wave-packets with particles, this phenomenon is known as Penrose process¹⁰ and for waves, it is called superradiant scattering¹¹ or Zel'dovich-Starobinsky effect¹². The explicit derivation can be done via the separation ansatz

$$\Phi_{\omega,\ell,m}(t, r, \vartheta, \varphi) = e^{-i\omega t + im\varphi} R_{\omega,\ell,m}(r) S_{\omega,\ell,m}(\vartheta). \quad (3)$$

Note that the applicability of this ansatz is non-trivial since the Kerr geometry does not factorize (hence the additional m -dependence). From the conversation of the Wronskian associated to the ordinary differential equation for $R_{\omega,\ell,m}(r)$, one can derive the following relation between the reflection (i.e., field amplitude at spatial infinity) and transmission (at the horizon) coefficients

$$1 - |\mathcal{R}_{\omega,\ell,m}|^2 = \frac{\omega - m\Omega_h}{\omega} |\mathcal{T}_{\omega,\ell,m}|^2, \quad (4)$$

where $\Omega_h = a/(2Mr_+)$ is the angular (frame-dragging) velocity at the horizon. Consequently, for the so-called anomalous modes with $\omega < m\Omega_h$, the reflection coefficient is larger than unity, i.e., the reflected wave is *stronger* than the incident one. Of course, this energy gain is taken from the gravitational (mainly rotational) energy of the black hole, which is diminished by back-reaction effects (remember that the in-falling part had an effectively negative energy). Enclosing the black hole by a large ideal mirror reflecting the amplified modes back into the ergo-region would then generate a blow-up instability¹¹ (“black-hole bomb”).

B. Unruh Effect

For non-rotating black holes, the negative energies do only occur inside the horizon and hence cannot be exploited in such a way, if we stay on the classical level. For quantum fields, however, the local positivity of the energy density is a much more subtle issue and the negative-energy states inside the horizon *can* be exploited by quantum effects – such as Hawking radiation. However, before turning to this striking phenomenon, let us study another quantum effect first.

The Minkowski vacuum is (per definition) empty, i.e., free of particles, for all observers/detectors at rest and also (via its Lorentz invariance) for all inertial observers/detectors moving with a constant velocity. Interestingly, this situations changes in the presence of acceleration a . Let us consider a uniformly accelerated trajectory, see Fig. 1. Evaluating the proper (co-moving wrist-watch) time along this trajectory we have to account for the constantly changing Lorentz boost factor

$$\tau = \int dt \sqrt{1 - \frac{\dot{x}^2(t)}{c^2}} = \frac{\text{arsinh}(at/c)}{a/c}. \quad (5)$$

Since the dynamics of a detector moving along this trajectory is governed by its proper time τ , the (linear) response of the detector can be inferred from the auto-correlation function in the Minkowski vacuum $|\text{vac}\rangle$

$$\langle \text{vac} | \hat{\Phi}(\tau) \hat{\Phi}(\tau') | \text{vac} \rangle = -\frac{a^2}{8\pi^2} \frac{1}{\cosh(a[\tau - \tau']/c) - 1}. \quad (6)$$

This expression is periodic along the imaginary proper time-axis $\tau \rightarrow \tau + 2\pi ic/a$, which motivates a thermal response of the detector. Indeed, it can be shown quite generally that a uniformly accelerated detector experiences the inertial vacuum state as a thermal bath with the Unruh temperature¹³

$$T_{\text{Unruh}} = \frac{\hbar}{2\pi k_{\text{B}} c} a = \frac{\hbar c}{2\pi k_{\text{B}}} \frac{1}{d_{\text{horizon}}}, \quad (7)$$

where $d_{\text{horizon}} = c^2/a$ is the horizon size, i.e., the minimum distance between the trajectory and the causally disconnected region (left Rindler wedge), see Fig. 1. The horizon experience by the accelerated observer is also the underlying reason for the thermal nature of the detector response: The Minkowski vacuum $|0_{\text{Min}}\rangle$ is a multi-mode squeezed state containing pairs of particles in either Rindler wedge

$$|0_{\text{Min}}\rangle = \exp \left\{ \int_{\mathbf{k}} e^{-\pi\omega/a} \hat{a}_{\text{R, left}}^\dagger(\omega) \hat{a}_{\text{R, right}}^\dagger(\omega) \right\} |0_{\text{FR}}\rangle, \quad (8)$$

where $\omega = \omega(\mathbf{k}) > 0$ is understood. Here $|0_{\text{FR}}\rangle$ denotes the Fulling-Rindler vacuum, which is the local ground state of the accelerated detectors. Since the accelerated observer cannot see the left Rindler wedge, we may trace over the degrees of freedom of the left wedge, which turns the pure state $|0_{\text{Min}}\rangle$ into a mixed state – which precisely corresponds to a thermal density matrix (thermo-field formalism¹⁴).

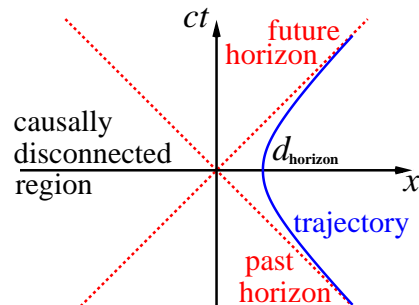


FIG. 1: Space-time trajectory with uniform acceleration and the associated horizons as boundaries of the Rindler wedges. No light ray (45°-lines) intersecting with the trajectory can reach the left wedge, which is causally disconnected.

C. Hawking Radiation

The Unruh effect described above is strongly related to Hawking radiation² via the principle of equivalence. In fact, Bill Unruh¹³ discovered it when trying to understand black hole evaporation. Imagine an imprudent astronaut freely falling towards (and finally through) the horizon. Locally, this freely falling astronaut is equivalent to an inertial observer. Another astronaut staying at a fixed distance to the horizon, however, feels the gravitational pull and thus corresponds to a uniformly accelerated observer. Now he/she can compare measurements results with his/her unfortunate colleague. Assuming that the freely falling astronaut does not experience anything special when passing the horizon, i.e., sees a quantum state locally equivalent to the Minkowski vacuum (as one would expect), the results of the previous section indicate that the stationary observer should see a thermal spectrum. Indeed, assuming a regular quantum state, the black hole emits thermal radiation with the Hawking temperature

$$T_{\text{Hawking}} = \frac{1}{8\pi M} \frac{\hbar c^3}{G_N k_B} = \frac{\hbar}{2\pi k_B c} a_{\text{surface gravity}}, \quad (9)$$

where the surface gravity measures the gravitational acceleration at the horizon, see the following table:

Unruh effect	Hawking effect
flat space-time	black hole
accelerated observer observer at a fixed distance	
inertial observer	freely falling observer

However, in spite of the analogy sketched above, there are also crucial differences between the Unruh effect and Hawking radiation: While the Unruh set-up is invariant under time-reversal (the acceleration remains unchanged after $t \rightarrow -t$), the Hawking scenario breaks this symmetry – one can only fall into the black hole, but never come out (see Sec. IID below). As a consequence, the Unruh effect is associated to a truly thermal bath containing an equal amount of particles in both directions and thus no net flux. In contrast, Hawking radiation corresponds to a real energy out-flux (black hole evaporation) and does not generate particles propagating from spatial infinity into the black hole. Furthermore, propagating the particles of the Hawking radiation back in time and thereby undoing the gravitational red-shift, we find that they originate from modes with shorter and shorter wavelengths in the past. Within the framework of quantum fields in classical curved space-times, there is no limit to this time-reversed squeezing process and thus these modes originate from an energy region (perhaps the Planck scale) where this semi-classical treatment breaks down and effects of quantum gravity become important. Ergo, Hawking's prediction is based on the extrapolation of a theory (quantum fields in

classical curved space-times) into an energy region where it is expected to break down. This observation poses the question of whether the Hawking effect survives after incorporating the effects of quantum gravity at high energies (trans-Planckian problem).

Let us study this question by implementing a change of the dispersion relation $\omega = ck \rightarrow \omega(k)$ as a toy model¹⁵ for high-energy deviations from classical general relativity. Using the Eddington-Finkelstein coordinates

$$ds^2 = \left(1 - \frac{2M}{r}\right) dv^2 - 2dv dr, \quad (10)$$

the wave equation of a massless scalar field reads

$$\left(2\partial_v \partial_r + \partial_r \left[1 - \frac{2M}{r} + f(-\partial_r^2)\right] \partial_r\right) \Phi = 0, \quad (11)$$

where we have added a modification $f(k^2)$ of the dispersion relation. After a Fourier-Laplace transformation, we get the following integral equation

$$(2\omega - k [1 + 2iM\partial_k^{-1} + f(k^2)]) \phi_\omega(k) = 0, \quad (12)$$

which can be solved via separation of variables

$$\phi_\omega(r) = \int \frac{dk}{g(k)} \exp \left\{ ikr - 2iM \int \frac{dk'}{g(k')} \right\}, \quad (13)$$

with the spectral function $g(k) = 1 + f(k^2) - 2\omega/k$. The integrand becomes singular at k_* where $g(k_*) = 0$, which is just the solution of the dispersion relation far away from the black hole $r \rightarrow \infty$. Assuming that $f(k^2)$ is an analytic function, we may calculate the integral by deforming the integration contour into the complex plane¹⁶. Since M is supposed to be very large (compared to the Planck mass and ω etc.), we may use the saddle-point method. We get two saddle points at large and real wavenumbers of opposite sign k_\pm , which are (as one would expect) solutions of the dispersion relation for finite r . These are the in-modes $\phi_{\text{in}}^\pm(\omega)$ and we shall assume that these short-wavelength modes are in their ground state $\hat{a}_{\text{in}}(\omega)|\text{in}\rangle = 0$. Finally, for closing the integration contour, we have to circumvent the branch cut originating from the singularity at k_* , which just yields the outgoing long-wavelength Hawking modes ϕ_{out} at $r \rightarrow \infty$. Now we may calculate the particle content in these out-modes ϕ_{out} by connecting them to the in-modes $\phi_{\text{out}}(\omega) \leftrightarrow \alpha_\omega \phi_{\text{in}}^+(\omega) + \beta_\omega \phi_{\text{in}}^-(\omega)$. The Bogoliubov coefficient can be obtained by comparing the saddle-point contributions at k_+ and k_- and determine the particle number via $\hat{a}_{\text{out}}(\omega) \leftrightarrow \alpha_\omega \hat{a}_{\text{in}}(\omega) + \beta_\omega \hat{a}_{\text{in}}^\dagger(\omega)$ which implies $\langle \text{in} | \hat{a}_{\text{out}}(\omega) \hat{a}_{\text{out}}^\dagger(\omega) | \text{in} \rangle = |\beta_\omega|^2$. Comparison with the Bose-Einstein distribution yields the effective Hawking temperature for each frequency¹⁷

$$T_{\text{Hawking}}(\omega) = \frac{v_{\text{gr}}(k_*) v_{\text{ph}}(k_*)}{8\pi M}, \quad (14)$$

where k_* denotes the solution of the dispersion relation for a given ω far away from the black hole $r \rightarrow \infty$

while v_{gr} and v_{ph} are the group and phase velocities at that frequency. If the dispersion relation becomes linear $\omega = ck$ at small k or approaches that of a massive particle $\omega^2 = m^2c^4 + c^2k^2$, we reproduce Eq. (9). However, if the dispersion relation $\omega(k)$ rises too fast (i.e., faster than quadratic), we would get an increasing amount of radiation at high energies (“UV-catastrophe”) and the black hole would evaporate quickly. Such a case should be excluded in view of our observational evidence of black holes with macroscopic life-times.

D. Eardley Instability and Black-hole Laser

After altering the dispersion relation, the Hawking particles do no longer originate from modes with arbitrarily short wavelengths squeezed against the horizon. Depending on the curvature of the dispersion relation, the short-wavelength modes are faster (superluminal case) or slower (subluminal case) than the speed of light c . Hence the in-modes with k_{\pm} approach the horizon from the inside (superluminal case) or the outside (subluminal case). During that process, they are stretched due to the gravitational red-shift (tidal forces) and their wavelength grows, i.e., their group and phase velocity approaches c . Finally, they are ripped apart by the horizon and one part (the Hawking particle) escapes to infinity while the remaining part (the in-falling partner particle) is trapped. This the in-falling partner particle has a negative energy (cf. Sec. II A) and thereby compensates the energy emitted by the Hawking radiation.

As mentioned above, this process is not symmetric under time-reversal. Now let us consider the time-reversed situation: Time-reversal turns a black hole (where nothing can escape) into a white hole (which nothing can penetrate). White holes are unstable solutions of the Einstein equations – while they still exert the gravitational attraction to everything, they do not allow anything to pass the white-hole horizon. Naturally, this leads to a pile-up at the horizon (until the dispersion relation changes or non-linear effects set in). Repeating the same analysis as before, we find that an in-going low-wavenumber vacuum state is transformed to outgoing high-wavenumber excitations. This means that white holes would decay very rapidly or turn into black holes (Eardley instability¹⁸).

Another interesting effect may occur when a black-hole horizon is combined with a white-hole horizon, which effectively happens in the Reissner-Nordström metric describing a charged black hole. In this case, the negative-energy wave packet may bounce back and forth between the two horizons where it emits a Hawking wave each time it hits the black-hole horizon and thereby constantly grows (similar to the “black-hole bomb” in Sec II A). This instability is called a black-hole laser¹⁹.

E. Cosmological Particle Creation

The phenomenon of particle creation is not restricted to the gravitational field around black (or white) holes, but may also occur in an expanding (or contracting) universe. Let us specify the action of a scalar field

$$\mathcal{A} = \frac{1}{2} \int d^4x \sqrt{|\mathbf{g}|} [(\partial_{\mu}\Phi)\mathbf{g}^{\mu\nu}(\partial_{\nu}\Phi) - \zeta\mathfrak{R}\Phi^2], \quad (15)$$

for the Friedmann-Robertson-Walker metric

$$ds^2 = \mathbf{a}^6(t)dt^2 - \mathbf{a}^2(t)d\mathbf{r}^2, \quad (16)$$

where $\mathbf{a}(t)$ is the time-dependent scale factor of the Universe and \mathfrak{R} the Ricci curvature scalar (ζ is the dimensionless curvature coupling factor, e.g., $\zeta = 1/6$ for conformal coupling in 3+1 dimensions and $\zeta = 0$ for minimal coupling). The wave equation reads

$$\ddot{\Phi}_{\mathbf{k}} + [\mathbf{a}^4(t)\mathbf{k}^2 + \zeta\mathbf{a}^6(t)\mathfrak{R}(t)]\Phi_{\mathbf{k}} = 0. \quad (17)$$

Accordingly, each \mathbf{k} -mode behaves as a harmonic oscillator with a time-dependent potential $\Omega_{\mathbf{k}}^2(t)$ given by $\Omega_{\mathbf{k}}^2(t) = \mathbf{a}^4(t)\mathbf{k}^2 + \zeta\mathbf{a}^6(t)\mathfrak{R}(t)$. Now, if the temporal variation of $\Omega_{\mathbf{k}}(t)$ is much slower than the internal frequency ($\dot{\Omega}_{\mathbf{k}} \ll \Omega_{\mathbf{k}}^2$ and $\ddot{\Omega}_{\mathbf{k}} \ll \Omega_{\mathbf{k}}^3$ etc.), the quantum state of the harmonic oscillator will stay near the ground state due to the adiabatic theorem. However, if the external time-dependence $\Omega_{\mathbf{k}}(t)$ generated by the cosmic expansion is too fast (i.e., non-adiabatic), the ground-state wave-function cannot adapt to this change anymore and thus the evolution will transform the initial ground state into an excited state in general (cosmological particle creation). Since Eq. (17) is linear, the excited state is a squeezed state

$$|\psi(t \uparrow \infty)\rangle = \exp \left\{ \sum_{\mathbf{k}} (\xi_{\mathbf{k}} \hat{a}_{\mathbf{k}} \hat{a}_{-\mathbf{k}} - \text{h.c.}) \right\} |0\rangle, \quad (18)$$

i.e., the particles are created in pairs of opposite wavenumbers due to momentum conservation.

Basically the same mechanism is (according to our standard model of cosmology) responsible for the generation of the seeds for structure formation out of the quantum fluctuations of the inflaton field. This process happened during inflation and at the end of this epoch, the amplified (squeezed) quantum fluctuations were transformed into density/temperature variations via the decay of the inflaton field. Traces of these primordial density/temperature variations can still be observed today in the anisotropies of the cosmic microwave background radiation.

F. Gibbons-Hawking Effect

In contrast to cosmological particle creation discussed above, where the produced particles can be detected *after*

the expansion, the Gibbons-Hawking effect²⁰ concerns the response of a detector *during* the expansion and is more similar to the Unruh effect. In order to point out the difference, let us rewrite the Friedmann-Robertson-Walker metric (16) in terms of the conformal time η

$$ds^2 = \mathbf{a}^2(\eta)[d\eta^2 - d\mathbf{r}^2], \quad (19)$$

and consider a conformally invariant field, e.g., massless scalar field in 1+1 dimensions or the electromagnetic field in 3+1 dimensions

$$\mathcal{A}_{\text{matter}} = -\frac{1}{4} \int d^4x \sqrt{-g} F_{\mu\nu} F^{\mu\nu}, \quad (20)$$

where $F_{\mu\nu}$ is the field strength tensor

$$F_{\mu\nu} = \nabla_\mu A_\nu - \nabla_\nu A_\mu = \partial_\mu A_\nu - \partial_\nu A_\mu. \quad (21)$$

The last equality exploits the symmetry of the Christoffel symbols $\Gamma_{\mu\nu}^\rho = \Gamma_{\nu\mu}^\rho$. Inserting the metric (19) into the action (20), we see that all factors of $\mathbf{a}(\eta)$ cancel and thus the field modes in terms of η are just undisturbed plane waves. Consequently, there is no cosmological particle creation in the sense of Sec. II E (conformal vacuum). However, this does not mean that a photon detector in such an expanding Universe would not click. In contrast to the photon modes, the detector dynamics is not labeled by the conformal time η but by the proper time $d\tau^2 = \mathbf{a}^2(\eta)d\eta^2$. Similar to Sec. II B, the two-point correlation function $\propto 1/(\eta - \eta')^2$ along the detector's trajectory $\mathbf{r} = 0$ changes after transformation to the proper time τ and hence the detector will detect excitations in general. For example, in the de Sitter Universe $\mathbf{a}(\tau) = \exp\{\mathfrak{H}\tau\}$ possessing a constant Hubble parameter $\mathfrak{H} = \dot{\mathbf{a}}/\mathbf{a}$, the auto-correlation function of the detector behaves as $\eta\eta'/(\eta - \eta')^2$, where the scale factors $\mathbf{a}(\eta)\mathbf{a}(\eta') = 1/\eta\eta'$ stem from the coupling to the physical degrees of freedom of the detector. In terms of the proper time $\tau \propto \ln \eta$, this translates into $\propto 1/\sinh^2(\mathfrak{H}[\tau - \tau'])$, which is analogous to Eq. (6). Again, we observe a periodicity in imaginary τ -direction and hence expect a behavior analogous to Unruh effect. Indeed, it can be shown²⁰ that the proper-time detector experiences the conformal vacuum as a thermal bath with a temperature

$$T_{\text{Gibbons-Hawking}} = \frac{\hbar}{2\pi k_{\text{B}}} \mathfrak{H}. \quad (22)$$

G. Schwinger Mechanism

It is instructive to identify common features of the various effects considered above. Apart from first example in Sec. II A (and, in some sense, the one in Sec. II D), they are pure quantum effects which do not occur on the classical level. E.g., the classical vacuum $\Phi \equiv 0$ remains empty $\Phi \equiv 0$ for all non-inertial observers. Furthermore, the effects in Sec. II A (and II D, of course) do also have their

quantum analogues: For quantized fields, it is not necessary to send a wave-packet into the rotating black hole in order to obtain superradiance, the in-going vacuum fluctuations are sufficient to create outgoing radiation. In all of these quantum effects, the in-going “virtual” quantum vacuum fluctuations are converted into “real” (w.r.t. the detector under consideration) particle pairs by the external influence (e.g., the gravitational field). These pairs are correlated (even entangled) and can be described by a (multi-mode) squeezed state such as in Eq. (8). For cosmological particle creation, the two particles have opposite momenta, cf. Eq. (18), whereas, for the Unruh effect, they live in distinct Rindler wedges, i.e., on different sides of the horizon. The same is true for the Gibbons-Hawking effect and the black-hole case in Sec. II C (as well as Sec. II A). In the latter situation each pair consists of an outgoing (Hawking) particle and its in-falling partner (with negative energy).

In addition, all of our examples are relativistic quantum effects. Thus, for typical laboratory parameters, these effects are suppressed due to large value of c and the smallness of \hbar (and partly G_N). Finally, for stationary scenarios, the effects mentioned above can be understood in terms of the population of negative energy states (which liberates the energy necessary for creating a “real” particle).

From this point of view, there is yet another effect, which also fits into this scheme: the Schwinger mechanism²¹⁻²⁵. In analogy to the gravitational field, which rips apart the wave packet near the horizon, a strong enough electric field may also pull an electron-positron pair out of the vacuum. This pair creation induced by the strong electric field is the main mechanism for neutralization of charged black holes (i.e., it is stronger than Hawking radiation for significantly charged black holes). However, it is not tied to black holes and might also occur in the laboratory. Let us consider a constant electric field $\mathbf{E} = Ee_x$ for simplicity. In this case, the dispersion relation of the electrons/positrons reads

$$(\omega \pm qEx)^2 = m^2 + k^2. \quad (23)$$

As a result, a classical electron trajectory with a given positive energy ω is incident from the right and then totally reflected (at the classical turning point). Positrons can be pictured as holes in the Dirac sea²¹ (corresponding to negative-energy states) and hence obey the opposite behavior, i.e., they are incident from the left and totally reflected back to the left. The two sets of classical trajectories are separated by the gap between the positive and negative energy states. For $E = 0$, this gap is given by $\omega_{\text{pos}} \geq +m$ and $\omega_{\text{neg}} \leq -m$. In the presence of an electric field $E > 0$, however, the gap is tilted and becomes x -dependent – which just correspond to the two classical turning points. In a quantum description, however, an electron from the Dirac sea may tunnel through the gap and become a real particle – leaving behind a hole, i.e., a positron. If the field E is not too strong, we may estimate the tunneling probability via the WKB

approximation. For $\omega = k_y = k_z = 0$, we get the eikonal of the exponential tail in the classically forbidden region in analogy to tunneling through a barrier from Eq. (23)

$$\int_{-m/(qE)}^{+m/(qE)} dx \sqrt{m^2 - (qEx)^2} = \pi \frac{m^2}{2qE}. \quad (24)$$

Hence the tunneling probability is exponentially suppressed $\propto \exp\{-\pi E_S/E\}$, where $E_S = m^2/q$ is called the Schwinger limit. At that ultra-high field strength, the work done separating the electron-positron pair over a Compton wavelength is of the order of the binding energy $2m$ and higher-order processes become important, i.e., the above estimate fails.

III. LABORATORY ANALOGUES

The effects sketched in the previous sections are fundamental predictions of quantum field theory in non-trivial (e.g., gravitational) background configurations. Testing these predictions would be extremely interesting – but, unfortunately, none of these effects has been directly observed yet. (So far, there are only indirect signatures, such as the anisotropies of the cosmic microwave background radiation mentioned in Sec. II E.) This lack of experimental evidence is mainly due to the suppression of these effects by the smallness of \hbar and $1/c$ and the resulting difficulty of creating strong enough fields or accelerations etc. One way of overcoming these obstacles are analogues using sound waves (or other quasi-particles) instead of photons (or electrons/positrons) and thereby effectively replacing the speed of light c by the speed of sound $c_s \lll c$. Of course, it would also be very interesting to find scenarios with an effectively increased \hbar in addition, but this option will not be discussed here.

A. The Acoustic Analogy

Analogies between laboratory systems and gravitational fields have been known for a long time (e.g., the Gordon metric²⁶), but it was probably Bill Unruh²⁷ who first realized that one could exploit these similarities for studying fundamental effects such as Hawking radiation. He considered sound waves $\delta\mathbf{v} = \nabla\Phi$ in irrotational fluids $\nabla \times \mathbf{v} = 0$, which obey the wave equation

$$\left(\frac{\partial}{\partial t} + \nabla \cdot \mathbf{v}_0\right) \frac{\varrho_0}{c_s^2} \left(\frac{\partial}{\partial t} + \mathbf{v}_0 \cdot \nabla\right) \Phi = \nabla \cdot (\varrho_0 \nabla\Phi) \quad (25)$$

where ϱ_0 and \mathbf{v}_0 denote the density and the velocity of the background flow and c_s is the speed of sound. The analogy to gravity is based on the striking observation that this wave equation is quantitatively equivalent to the d'Alembertian in a curved space-time

$$\square_{\text{eff}}\Phi = \frac{1}{\sqrt{-g_{\text{eff}}}} \partial_\mu (\sqrt{-g_{\text{eff}}} g_{\text{eff}}^{\mu\nu} \partial_\nu \Phi) = 0, \quad (26)$$

if the effective (acoustic) metric $g_{\text{eff}}^{\mu\nu}$ is chosen in a specific way, which is similar to the Painlevé-Gullstrand-Lemaître form²⁸ known from gravity

$$g_{\text{eff}}^{\mu\nu} = \frac{1}{\varrho_0 c_s} \begin{pmatrix} 1 & \mathbf{v}_0 \\ \mathbf{v}_0 & \mathbf{v}_0 \otimes \mathbf{v}_0 - c_s^2 \mathbf{1} \end{pmatrix}. \quad (27)$$

As a result, phonons propagating in this flowing fluid behave precisely in the same way as a scalar (quantum) field in a curved space-time described by the above metric. Even though the form (27) is not flexible enough to reproduce *all* possible gravitational fields (e.g., it cannot simulate the full Kerr geometry), it is sufficiently general to model rotating and non-rotating black or white holes (cf. Secs. II A, II C, and II D) and an expanding or contracting universe (cf. Sec. II E). The Unruh and the Gibbons-Hawking effect discussed in Secs. II B and II F, respectively, require a more detailed consideration of the phonon detector. Recreating the Schwinger mechanism necessitates the analogue of a Dirac sea and thus fermionic quasi-particles as well as the coupling to an electric field analogue. (An experiment along these lines has been done in graphene²⁹. However, the quasi-particle spectrum does not exhibit a mass gap in this system and hence the analogy to the Schwinger mechanism is limited.)

B. Further Analogues

The analogy between condensate matter and gravity is not restricted to sound waves, it may apply to other quasi-particles as well. If the quasi-particles are Goldstone-modes (i.e., gap-less) and can be described by a single scalar field Φ , the most general linearized low-energy effective action reads³⁰

$$\mathcal{L}_{\text{eff}} = \frac{1}{2} (\partial_\mu \Phi) (\partial_\nu \Phi) G^{\mu\nu} + \mathcal{O}(\Phi^3) + \mathcal{O}(\partial^3), \quad (28)$$

where $G^{\mu\nu}$ is governed by the underlying condensed-matter system and may depend on space and time in general. Identifying $G^{\mu\nu} \rightarrow g_{\text{eff}}^{\mu\nu} \sqrt{|g_{\text{eff}}|}$, we again find a qualitative analogy to gravity. Apart from phonons, examples for such quasi-particles are surface waves (ripples) on top of flowing liquids³¹ or photons with a fixed polarization in wave guides³² or optical fibers³³. Under additional assumptions, the analogy can also be extended to non-scalar quasi-particles. One example are photons in a moving dielectric medium with an arbitrary four-velocity u^μ and a constant (scalar) permittivity ε , whose behavior is analogous to a curved space-time with the Gordon metric²⁶

$$g_{\text{eff}}^{\mu\nu} = g_{\text{Min}}^{\mu\nu} + (\varepsilon - 1) u^\mu u^\nu. \quad (29)$$

It is even possible to model the 1+1 dimensional Dirac equation (i.e., spin-1/2 particles) within a slow-light setup³⁴, but these excitations do still obey bosonic commutation relations, i.e., there is no Dirac sea.

C. Analogue Gravity

Let us apply the concepts and tools from general relativity to the acoustic metric (27); most of the other effective metrics are very similar. Comparing Eqs. (27) and (1), we see that an ergo-region occurs for supersonic flow velocities $v_0^2 > c_s^2$. A horizon, on the other hand, corresponds to a closed surface at which the *normal* flow velocity exceeds the speed of sound $v_\perp = c_s$. For a radial or effectively one-dimensional flow, the two points coincide, but for a maelstrom-type flow (which can still be locally irrotational), there is a finite ergo-region outside the horizon. Since the effective energy of the phonons may become negative in this region, we may obtain superradiance effects.

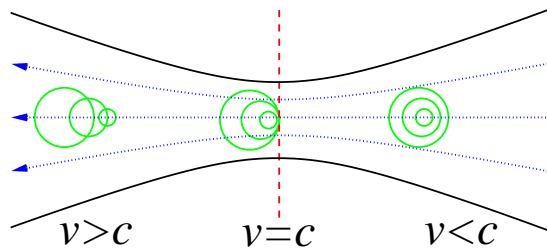


FIG. 2: Sketch of a de Laval nozzle as an analogue for a black hole. The solid (black) lines denote the walls of the nozzle and the dotted (blue) curves are the streamlines of the flow. At the entrance of the nozzle (right), the flow is sub-sonic $v < c$. The flow velocity exceeds the speed of sound at the narrowest point and exits the nozzle (left) with a super-sonic velocity. The phonons are depicted by (green) circles. In the sub-sonic region (right), they may propagate in both directions – but in the supersonic part (left), they are swept away and cannot escape anymore. Hence the border (red dashed line) between the two regions is analogous to a black hole horizon with the right half of the nozzle corresponding to the outside of the black hole and left half modelling the black hole interior.

If the flow is accelerated (following a streamline) from subsonic to supersonic velocities (such as in a de Laval nozzle, cf. Fig. 2), we obtain the analogue of a black-hole horizon, which traps all sound waves. The time-reverse, i.e., a flow decelerated from supersonic back to subsonic speed, would correspond to a white-hole horizon, which expels all phonons. As one would expect from the discussion in Sec. II D, such a flow profile is typically plagued with instabilities (towards the generation of shock waves etc.).

Generating the analogue of a black hole horizon in a de Laval nozzle, for example, the same arguments as in Hawking’s original derivation² would imply a thermal phonon flux moving upstream. Even if we send in the fluid at zero temperature, the in-going quantum fluctuations of the phonon modes will be ripped apart by the horizon and generate excitations in the form of phonon pairs. (One phonon escapes to the entrance of the nozzle and the other one is swept away toward its exit.) Inserting the acoustic metric (27), the surface gravity is

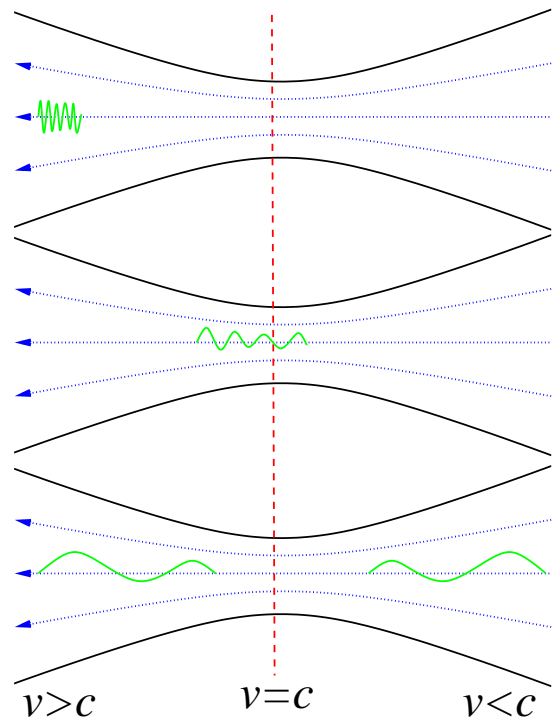


FIG. 3: Evolution of the wave-packet generating the Hawking radiation in a de Laval nozzle for a super-sonic dispersion relation. Initially, the short-wavelength wave-packet (k_\pm in Sec. II C) with a large group velocity $d\omega/dk > c$ is propagating upstream and approaches the horizon from the inside (top panel). During that process, the flow inhomogeneity stretches the wave-packet (middle panel) in analogy to the gravitational red-shift and thereby lowers its group velocity until $d\omega/dk \approx c$. Finally, the wave-packet is ripped apart by the horizon into two parts (bottom panel), the outgoing Hawking radiation (k_* in Sec. II C) and its in-falling partner (both with long wavelengths).

determined by the velocity gradient at the horizon and thus the Hawking temperature reads

$$T_{\text{Hawking}} = \frac{\hbar}{2\pi k_B} \left| \frac{\partial}{\partial r} (v_0 - c_s) \right|_{v_0=c_s}. \quad (30)$$

Inserting typical values for potential condensed matter analogues, we obtain relatively low temperatures – which are, however, still orders of magnitude larger than for astronomical black holes. Of course, the trans-Planckian problem does also play a role here, because the Hawking phonons originate from modes with very short wavelengths, where fluid dynamics breaks down. In contrast to (quantum) gravity, we do know (at least in principle) the correct microscopic theory for fluids – and thus we may address the trans-Planckian problem. If a change of the dispersion relation describes the relevant deviation from fluid dynamics at short length scales, we may employ the methods sketched in Sec. II C, cf. Fig. 3). Other effects (such as non-linear interactions), however, are much less understood.

Finally, the metric (27) can also model an expanding or

contracting universe. There are basically two possibilities (which can be combined): an expansion or contraction of the fluid and variations in the local speed of sound.

IV. LABORATORY SYSTEMS

Now, after having briefly discussed the underlying analogy, we are in the position to study some explicit condensed-matter examples. The following selection is not exhaustive, but aimed at providing a rough overview and indicating possible future directions.

A. Trapped Ions

Let us start with a system where the technology for cooling to the ground state and detecting single particles is most advanced – a chain of ions in a trap. Assuming that the radial confinement is very tight, it is sufficient to consider the positions q_i of the ions in axial direction. In the presence of a time-dependent harmonic axial trap potential ω_{ax}^2 , the equations of motion read³⁵

$$\ddot{q}_i(t) + \omega_{\text{ax}}^2(t)q_i(t) = \gamma \sum_{j \neq i} \frac{\text{sign}(i-j)}{[q_i(t) - q_j(t)]^2}, \quad (31)$$

where γ denotes the strength of the Coulomb repulsion. The classical equations of motion can be solved in terms of a single scale parameter given by

$$\ddot{b}(t) + \omega_{\text{ax}}^2(t)b(t) = \frac{\omega_{\text{ax}}^2(0)}{b^2(t)}. \quad (32)$$

In order to obtain the phonon modes, we split the full quantum position operator $\hat{q}_i(t)$ into the classical solution $b(t)q_i^0$ which is fully determined by the initial static position q_i^0 plus small (linearized) quantum fluctuations $\hat{q}_i(t) = b(t)q_i^0 + \delta\hat{q}_i(t)$. After linearization and normal-mode decomposition, we obtain the phonon modes

$$\left(\frac{\partial^2}{\partial t^2} + \omega_{\text{ax}}^2(t) + \frac{\omega_{\kappa}^2}{b^3(t)} \right) \delta\hat{q}_{\kappa} = 0, \quad (33)$$

where ω_{κ}^2 are the time-independent eigenfrequencies of the phonon modes labelled by κ . Identifying $\kappa \leftrightarrow \mathbf{k}$, $\omega_{\kappa}^2 \leftrightarrow \mathbf{k}^2$, $b(t) \leftrightarrow \mathbf{a}(t)$, $\omega_{\text{ax}}^2(t) \leftrightarrow \mathfrak{R}(t)$, we obtain a striking similarity to Eq. (17). Moreover, both, $\mathfrak{R}(t)$ and $\omega_{\text{ax}}^2(t)$, are related to the second time-derivatives of the corresponding scale factors $\mathbf{a}(t)$ and $b(t)$. As a result of the analogy between Eqs. (33) and (17), we obtain the analogue of cosmological particle creation in an ion trap with a time-dependent axial trapping strength $\omega_{\text{ax}}^2(t)$. Accordingly, the initial phonon creation and annihilation operators $\hat{a}_{\kappa}^{\dagger}(0)$ and $\hat{a}_{\kappa}(0)$ are related to the final phonon operators via the Bogoliubov transformation

$$\hat{a}_{\kappa}(t \uparrow \infty) = \alpha_{\kappa} \hat{a}_{\kappa}(0) + \beta_{\kappa} \hat{a}_{\kappa}^{\dagger}(0), \quad (34)$$

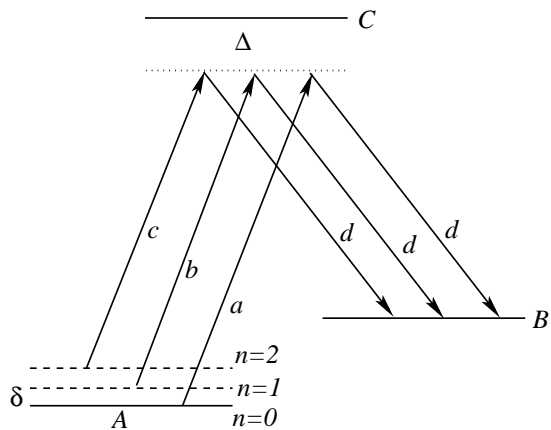


FIG. 4: Sketch (not to scale) of the relevant electronic (vertical solid lines) and motional (vertical dashed lines) levels and the associated transitions (arrows).

which exactly corresponds to the squeezed state in Eq. (18) via $|\alpha_{\kappa}\rangle \leftrightarrow \cosh(|\xi_{\mathbf{k}}|)$ and $|\beta_{\kappa}\rangle \leftrightarrow \sinh(|\xi_{\mathbf{k}}|)$.

The created phonon pairs can be detected via suitable red-sideband Raman transitions, see Fig. 4. Initially, the ions are in the electronic (A) and motional ground state ($n = 0$). Then applying a Raman π -pulse ($a + d$) would transfer the full population into the meta-stable state B without actually populating the excited state C due to the large detuning Δ . If we apply an additional detuning $n\delta$ to one of the Laser beams only, i.e., a first ($n = 1$) or second ($n = 2$) side-band transition $b + d$ or $c + d$, respectively, we may selectively transfer population from the excited motional levels $n = 1$ or $n = 2$ only to the state B. Since the occupation of that meta-stable state B could be measured by suitable detected by resonance fluorescence methods, we may infer the initial motional level. It is even possible to distinguish two-phonon states $n = 2$ from one-particle excitations $n = 1$, which could be used to discriminate the quantum effect (squeezed state with phonon pairs) from classical effects such as heating³⁵.

In contrast to the above analogue to cosmological particle creation in an ion trap, where the produced phonons are measured *after* varying the trap frequency $\omega_{\text{ax}}^2(t)$, there has been another proposal for detecting phonons *during* the expansion of the ion cloud³⁶. However, the latter proposal poses several technical and conceptual problems: Since the phonon modes are not conformally invariant, one would obtain some sort of combination of the Gibbons-Hawking effect and cosmological particle creation, cf. Eq. (34), which has not been taken into account sufficiently. Furthermore, resolving the phonon energies δ requires a sufficiently long measurement time $\Delta t = \mathcal{O}(\hbar/\Delta E) = \mathcal{O}(\hbar/\delta)$. Sustaining an exponential expansion during such a long time is of course very difficult. Finally, the ion dynamics (32) was not included adequately.

In summary, the analogue of cosmological particle creation should be realizable experimentally with present-day technology (in fact, the experimental efforts are al-

ready under way³⁵). Unfortunately, simulating the other quantum effects with this set-up seems to be more complicated. The main reason for these difficulties lies in the restricted parameter range (e.g., number and distance of ions) for which the coherent control can be maintained. As mentioned before, the advantages of this set-up lies in the ability to cool very close to the (motional plus electronic) ground state (better than 90%) and to detect single phonons.

B. Bose-Einstein Condensates

Another laboratory system capable of achieving very low temperatures experimentally is a Bose-Einstein condensate³⁷. In the dilute-gas limit, it can be described by the many-particle Hamiltonian density

$$\hat{\mathcal{H}} = \hat{\Psi}^\dagger \left(-\frac{\nabla^2}{2m} + V_{\text{ext}}(t, \mathbf{r}) + \frac{g}{2} \hat{\Psi}^\dagger \hat{\Psi} \right) \hat{\Psi}, \quad (35)$$

where m is the mass of the condensed particles (e.g., atoms) and $V_{\text{ext}}(t, \mathbf{r})$ the external trap potential. The coupling $g > 0$ describes the repulsion between the particles (in s -wave scattering approximation) and generates the internal pressure p . For dilute condensates consisting of many particles, the bosonic field operator can be approximately replaced by a c-number $\hat{\Psi} \approx \psi$ at low temperatures. The order parameter ψ corresponds to the macroscopically occupied wave function of the condensate and obeys the Gross-Pitaevskii equation

$$i\dot{\psi} = \left(-\frac{\nabla^2}{2m} + V_{\text{ext}}(t, \mathbf{r}) + g|\psi|^2 \right) \psi. \quad (36)$$

Inserting the Madelung split $\psi(t, \mathbf{r}) = \sqrt{\varrho(t, \mathbf{r})} e^{iS(t, \mathbf{r})}$ into density ϱ and phase S , we obtain the equation of continuity $\dot{\varrho} + \nabla \cdot (\varrho \mathbf{v}) = 0$ for the condensate velocity $\mathbf{v} = \nabla S/m$ and the Hamilton-Jacobi equation

$$\dot{S} + V_{\text{ext}} + g\varrho + \frac{(\nabla S)^2}{2m} = \frac{1}{2m} \frac{\nabla^2 \sqrt{\varrho}}{\sqrt{\varrho}}, \quad (37)$$

strongly resembles the Bernoulli equation apart from the term on the r.h.s. Indeed, on length scales much larger than the healing length $\xi = 1/\sqrt{mg\varrho}$, this term can be neglected and we obtain a fluid dynamic description at distances $\gg \xi$.

Therefore, the condensate can be described by an irrotational fluid. Vorticity may only occur via “drilling a hole” in the condensate, i.e., a vortex at which center the condensate density vanishes. Going around the vortex, the phase of the wave-function ψ changes by an integer multiple of 2π due to the single-valued character of the wave-function ψ . Therefore, the circulation is quantized according to $\Gamma = \oint d\mathbf{r} \cdot \mathbf{v} \in 2\pi\mathbb{N}/m$. On very large scales, however, a collection of many vortices seems to approach the classical Euler equation with rotation and even viscosity (shedding of phonons and vortex rings) including phenomena like turbulence (vortex tangle).

The equation of state can be inferred from (37) to be $p(\varrho) = g\varrho^2/(2m)$. Hence the sound velocity is given by $c_s^2 = g\varrho/m$ and the sound dispersion relation can be obtained by linearizing (37)

$$(\omega - \mathbf{v}_0 \cdot \mathbf{k})^2 = c_s^2 \mathbf{k}^2 + \left(\frac{\mathbf{k}^2}{2m} \right)^2 = c_s^2 \mathbf{k}^2 \left(1 + \frac{\xi^2}{4} \mathbf{k}^2 \right) \quad (38)$$

Thus, for dilute condensates, deviations from fluid dynamics at short wavelengths $\lambda \leq \mathcal{O}(\xi)$ manifest themselves in a departure of the dispersion relation from the phonon branch $c_s|\mathbf{k}|$ towards the free-particle behavior $\mathbf{k}^2/(2m)$. Apart from our good theoretical understanding of Bose-Einstein condensates (which is far less developed for most other fluids), they offer a high degree of experimental controllability: The external potential V_{ext} can be generated by laser beams and thus there are no walls³⁸ which might induce friction etc. One may even realize effectively lower-dimensional condensates (if the transversal length scales are far below the healing length ξ). Furthermore, Bose-Einstein condensates are coupled only very weakly to the environment, which allow us to reach extremely low temperatures (of order nano-Kelvin). Finally, for non-trivial topologies, one may generate persistent currents via trapping flux quanta imprinted on phase S .

Both, our good theoretical understanding and the high degree of experimental controllability, render Bose-Einstein condensates an ideal play-ground for theoretical and hopefully experimental investigations of the analogy to gravity. In fact, most of the studies so far have been devoted to this system: In time-of-flight experiments, one uses an expansion of the condensate cloud in order to spatially amplify the desired signal. On the classical level, the expansion can be described in terms of a scaling parameter similar to Eq. (32). The quantum fluctuations of the phonons, however, should imply effects analogous to cosmological particle creation resulting in frozen density (on the percent-level) variations similar to cosmic inflation^{39,40}. Alternatively, expanding or contracting universes can be modelled⁴⁰⁻⁴² by temporal variations of the coupling g (e.g., via a Feshbach resonance). It is even possible to simulate a change of the signature of the metric by switching from repulsive to attractive interactions⁴³ (which leads to a “Bose-nova” instability⁴⁴). For these effects, the healing length ξ in Eq. (38) provides a natural UV cut-off and allows us to study its impact on the spectrum of produced particles⁴⁵.

By inserting an atomic quantum dot as a detector model into the condensate, it is also possible to simulate the Gibbons-Hawking effect⁴⁶ in a condensate in one spatial dimension (remember that the scalar field is conformally invariant in 1+1 dimensions). Going a step further and moving the atomic quantum dot through the (otherwise static) condensate with a varying velocity, one may pick up excitations due to non-adiabatic response of the quantum fluctuations⁴⁷. This quantum effect is a bit similar to the Unruh effect, but there are important differences: The non-adiabatic response is caused by the

Doppler shift (and hence works in the desired way in a certain direction only) and not by a real Lorentz time dilatation as in (5).

Classical effects such as superradiance, the white-hole instability, and the black-hole laser have been observed numerically by simulating the Gross-Pitaevskii equation (36) and should also be accessible experimentally⁴⁸. For example, a multiply quantized vortex (which is known to be unstable) is surrounded by the analogue of an ergo-region as in the Kerr metric and superradiance-like effects should play a role in its decay.

In a two-component Bose-Einstein condensate, it is possible to mix the two species via optical transitions and thus to simulate a massive Klein-Fock-Gordon equation⁴⁹ via effectively breaking the $U(1) \times U(1)$ symmetry down to $U(1)$. This construction provides an example for the possible interplay between the cut-off scale and the mass scale⁵⁰.

Finally, for Hawking radiation in Bose-Einstein condensates⁵¹, the characteristic temperatures can be estimated from (30). Since the curved space-time analogy breaks down at length scales smaller than the healing length (typically below a micrometer) and the speed of sound is of order mm/s, we get a maximum Hawking temperature of order nano-Kelvin⁵². The detection of the small number of emitted phonons could in principle⁵³ be done with similar methods as described in Sec. IV A, cf. Fig. 4, but for Bose-Einstein condensates, this technology is not as far advanced as for ion traps. Another interesting idea for detecting the Hawking process is to look at density-density correlations across the horizon⁵⁴, which show characteristic peaks due to the entanglement between the Hawking radiation and their partner particles described by a multi-mode squeezed state as in (8). However, inserting typical values, these peaks are very weak and thus extremely hard to observe.

Unfortunately, besides the aforementioned advantages, Bose-Einstein condensates go along with a major drawback: All the gaseous condensates realized in the laboratory are only meta-stable states – the true ground state is a solid. The main decay channels of the gaseous state are (inelastic) three-body collisions. Such an event transforms three indistinguishable bosons from the cloud into a molecule plus a remaining boson which carries away the large excess energy/momentum – and thereby all three of them are effectively extracted from the condensate (formed of low-energy bosons). Now, if all three of these bosons stem from the same macroscopically occupied single-particle wave-function ψ of the condensate ($\mathbf{k} = 0$), three-body collisions would just slowly diminish the number of condensed bosons. However, in the presence of inter-particle interactions $g > 0$ (which are necessary for the propagation of sound), the many-particle ground state does also contain a small population of the higher single-particle states $\mathbf{k} > 0$. This small fraction is called quantum depletion since it is generated by the quantum fluctuations (plus the interaction g). Thus, if one of the three bosons involved in the inelastic collision

stems from the quantum depletion and is removed, this event causes a deviation from the many-particle ground state – i.e., an excitation⁵⁵. Ergo, three-body collisions do also heat up the condensate, which might swamp the quantum signal to be detected⁵⁶. For example, considering a Bose-Einstein condensate containing 10^7 particles and 1% quantum depletion with 1% three-body losses (in total) during the experiment (which are already quite optimistic values), there would be $\mathcal{O}(10^3)$ noise phonons in addition to the weak Hawking signal. In order to avoid this problem (and other issues, such as the black hole laser instability), it is probably desirable to employ a very fast detection method.

C. Surface Waves

As mentioned in Sec. III B, the analogy to gravity is not limited to phonons but may apply to other quasi-particles as well. As one example, the propagation of surface waves (ripples) on top of locally irrotational flowing liquids corresponds to an effective metric very similar to Eq. (27) at long distances. This includes gravity waves (not to be confused with gravitational waves) in flowing water as well as third sound (i.e., surface waves) in liquid Helium (where gravity is replaced by van-der-Waals forces).

As a result, the vortex flow which occurs when draining the bath tub, for example, exhibits similarities to a rotating black hole and some of the associated instabilities might be related to superradiance. As another scenario which can be realized in a sink, we may let the water jet from the tap impinge perpendicularly onto a flat surface (e.g., the sink bottom) and thereby generate a radial diverging flow. For suitable parameters, the radial flow is faster than the surface wave speed (i.e., “superluminal”) in the middle and becomes slower (“subluminal”) at some given radius. This point corresponds to a white-hole horizon⁵⁷ and is known as hydraulic jump in view of the instabilities occurring there: the quasi-regular radial flow in the middle becomes irregular beyond that radius and the water height changes abruptly (jump). The instabilities generating this phenomenon are probably related to the Eardley effect.

A similar experiment has been carried out in a water tank⁵⁸ which was quite large (in order to minimize viscosity effects etc.) and allowed the quantitative determination of the mixing of positive $\phi_{\text{out}}^+(\omega)$ and negative $\phi_{\text{out}}^-(\omega)$ frequency modes $\alpha_\omega \phi_{\text{out}}^+(\omega) + \beta_\omega \phi_{\text{out}}^-(\omega) \leftrightarrow \phi_{\text{in}}(\omega)$ roughly analogous to the time-reversed Hawking process, cf. Sec. II C. However, the measured results α_ω and β_ω did not match the expected values and the curved space-time analogy probably does not apply quantitatively to this experiment.

In summary, the simulation of classical effects with surface waves is potentially difficult but in principle possible – while it is hard to see how analogues of quantum phenomena could be detected.

D. Optical Fibers and Wave-Guides

In order to model a black hole horizon for electromagnetic waves in the same way as in the previous sections, the velocity of the medium should exceed the speed of light in that medium⁵⁹ at some point, cf. Eq. (29). Unless one uses meta-materials or other slow-light media (which induce further problems³⁴), this is very difficult to realize experimentally. Therefore, one may chose an alternative route: Instead of actually moving the medium, one could send a pulse (representing a phase boundary) through the medium such that the speed of light in front of the pulse is larger than its velocity of propagation – whereas the speed of light behind the pulse is smaller. Transforming to the inertial reference frame co-moving with the pulse, we see that it also corresponds to a black hole horizon.

This scenario facilitates much larger velocities and hence higher Hawking temperatures, cf. Eq. (30). For electromagnetic wave-guides³² supporting radio or micro waves, the Hawking temperature could range up to fractions of a Kelvin. For optical fibers³³, the value could be even larger. However, for normal non-linear optical media (where the refractive index increases with intensity), the Kerr effects tends to make the front end of a light pulse (i.e., the black hole horizon) flat and its rear end (i.e., the white hole horizon) steep. As a result, the effective surface gravity for the black hole horizon (and hence the Hawking temperature) becomes rather small while the effective surface gravity for the white hole horizon is increased. For this reason, the recent experiment in optical fibers³³ considered the white hole horizon and measured the classical mixing of positive $\phi_{\text{out}}^+(\omega)$ and negative $\phi_{\text{out}}^-(\omega)$ frequency modes $\alpha_\omega \phi_{\text{out}}^+(\omega) + \beta_\omega \phi_{\text{out}}^-(\omega) \leftrightarrow \phi_{\text{in}}(\omega)$ roughly analogous to the time-reversed Hawking process, cf. Sec. II C.

One of the main advantages of these electromagnetic scenarios lies in the fact that the amplification and detection of photons (in the relevant energy range) is much easier than in the case of phonons. Nevertheless, observing quantum effects is still quite hard because the small signal to be detected arrives just before the huge pulse (in the black hole case) or, even worse, just after the pulse (for white hole analogues).

E. Ultra-intense Lasers and the Unruh Effect

In all of the previous example, the speed of light in vacuum has been effectively replaced by the reduced propagation velocity of quasi-particles (such as phonons, ripples, or photons) in a medium. In the following, we shall discuss a scenario where this is not the case and consider a real relativistic quantum effect. With modern lasers, it is possible to reach extremely high intensities via suitable focussing techniques⁶⁰. Electrons under the influence of these strong electric fields would undergo an immense acceleration and thus experience the Minkowski vacuum as a thermal state with a relatively large temperature⁶¹.

However, the electron is not a good photon detector since it cannot absorb a photon while passing to an excited internal state – and thus directly observing the Unruh effect is rather difficult. On the other hand, the electron *can* scatter photons from one into another mode via Thomson (or Compton) scattering. Consequently, switching to the accelerated frame co-moving with the electron, there is a finite probability that the electron scatters a (“virtual”) photon out of the thermal bath into another mode. In terms of the squeezed state in Eq. (8), this corresponds to $\hat{a}_{\text{R, right}}^\dagger(\mathbf{k})\hat{a}_{\text{R, right}}(\mathbf{k}')|0_{\text{Min}}\rangle$ with $\omega(\mathbf{k}) = \omega(\mathbf{k}')$ due to energy conservation (in the accelerated frame). Translation back into the inertial frame yields the creation of an entangled *pair* of photons out of the quantum vacuum fluctuations due to the non-inertial scatterer. This result can be understood in the following way: Since the Minkowski vacuum is annihilated by a linear combination of Rindler operators in the left and right wedges¹³

$$\left(e^{-\pi\omega/a}\hat{a}_{\text{R, left}}^\dagger(\omega) + \hat{a}_{\text{R, right}}(\omega)\right)|0_{\text{Min}}\rangle = 0, \quad (39)$$

removing one Rindler particle $\hat{a}_{\text{R, right}}(\mathbf{k}')|0_{\text{Min}}\rangle$ from the right wedge (e.g., via absorption by the accelerated detector) leaves its partner particle in the left wedge behind $\hat{a}_{\text{R, left}}^\dagger(\omega)|0_{\text{Min}}\rangle$ and thereby liberates it to become a real excitation⁶². Furthermore, inserting an additional particle into the right wedge $\hat{a}_{\text{R, right}}^\dagger(\mathbf{k})|0_{\text{Min}}\rangle$ does also cause a deviation from the vacuum state $|0_{\text{Min}}\rangle$ and thus corresponds to a real excitation, i.e., photon.

The created photon pairs may then serve as a signature of the Unruh effect and their entanglement (e.g., in polarization⁶³) reflects the correlations between the left and right Rindler wedge, cf. Eq. (8). As stated before, these correlations across the horizon are genuine features of the considered quantum effects such as Hawking radiation. The two-photon nature of these signatures of the Unruh effect should (at least in principle) allows us to distinguish it from other effects such as classical Larmor radiation (given off by all accelerated charges).

For a close analogy to the Unruh effect (uniform acceleration), one would like to have a very strong and approximately constant electric field and a negligible magnetic field. However, it is rather hard to obtain a strong enough quantum signal in this set-up and to distinguish it from the classical background. A stronger signal and better discrimination from Larmor radiation could be achieved via an alternative scenario, which does, however, no longer correspond to uniform acceleration: Colliding an ultra-relativistic electron beam with a counter-propagating laser pulse, the electric field felt by the electrons and hence their acceleration is strongly amplified by the Lorentz boost factor. Furthermore, the quantum (Unruh) signal and the classical (Larmor) background are better separated in phase space (energy and momentum) in this situation⁶³.

Finally, it should be mentioned that there are also further indirect signatures of the Unruh effect⁶⁴, some

of them have already been observed. For example, the residual polarization variance of electrons in accelerator rings can partly be attributed to the Unruh effect⁶⁵: The orbiting electron is constantly (though not uniformly) accelerated and thus experiences the Minkowski vacuum as a nearly thermal bath, which inhibits a perfect polarization⁶⁵. Another example are accelerated atoms in a cavity⁶⁶. However, in this scenario, the main signal is not generated by the actual acceleration of the atom, but by non-adiabatic switching effects. Therefore, this set-up displays more similarities to the ion-trap configuration in Sec. IV A.

F. Schwinger Mechanism in the Laboratory?

With the laser systems currently under preparation⁶⁷, it should become possible to approach the Schwinger limit E_S within two orders of magnitude in the focus of the high-intensity laser. Via high-harmonic focusing⁶⁸, it may even be possible to reach much higher intensities. Therefore, the experimental observation of the Schwinger mechanism, which is a non-perturbative QED vacuum effect, may become within reach in the near future. Note that its non-perturbative character clearly distinguishes the Schwinger mechanism from perturbative (multi-photon) pair-creation effects, which have already been observed in accelerators.

However, since it is probably rather hard to actually reach the Schwinger limit E_S and the pair-creation rate is exponentially (non-perturbatively) suppressed $\propto \exp\{-\pi E_S/E\}$, it is desirable to increase the signal. As one possibility, one could superimpose the strong and slow electric field with weak and fast electromagnetic wiggles of frequency $\Omega < m$. Even though these wiggles cannot produce electron-positron pairs directly, they help the “virtual” electrons to penetrate into the gap and thus decrease the distance between the classical turning points $x_{\pm} = \pm(m - \Omega)/(qE)$. As a result, the tunnelling exponent in Eq. (24) is altered to

$$\int_{x_-}^{x_+} dx \sqrt{m^2 - (qEx - \Omega)^2} = \frac{m^2}{4qE} \times f\left(\frac{\Omega}{m}\right), \quad (40)$$

with $f(\chi) = \pi + 2 \arcsin(1 - 2\chi) + 4\sqrt{\chi}(1 - 2\chi)\sqrt{1 - \chi}$, which can be approximated by $f(\chi) \approx 2\pi(1 - \chi)$ in the relevant interval $\chi \in [0, 1]$. Consequently, the tunnelling exponent can be decreased by the weak and fast electromagnetic wiggles⁶⁹, e.g., for $\chi = 1/2$, the pair-creation rate scales with $\propto \exp\{-\pi E_S/(2E)\}$, which is a huge enhancement for $E \ll E_S$.

V. THE BIG PICTURE

Now, after having discussed various scenarios for recreating fundamental effect is the laboratory, let us turn to

the question of what we can learn from these considerations. First and foremost, these scenarios facilitate (at least in principle) an experimental test of the striking predictions of quantum field theory in non-trivial backgrounds. This allows us to test the methods, assumptions, and approximations underlying these predictions (cf. the trans-Planckian problem discussed in Sec. II C, for example). Furthermore, after detecting the desired effect itself, we might experimentally study corrections induced by interactions between the quasi-particles (which are theoretically not fully understood) as well as non-perturbative aspects (e.g., the Schwinger mechanism).

Apart from these experimental issues, the study of the laboratory analogues does also provide new ideas for investigating the possible microscopic structures of quantum gravity inspired by condensed matter. For example, the trans-Planckian issue can be approached via considering a change in the dispersion relation, cf. Sec. II C. These calculations suggest that (in the absence of a “UV-catastrophe”) Hawking radiation is basically a low-energy process. This observation casts some doubt on the frequently suggested resolution of the black hole information “paradox” postulating subtle correlations in the outgoing Hawking radiation which carry away the information. If the Hawking particles are created at low energies near the horizon, it is hard to see how they can be influenced by the information “stored” in the black hole, which is presumably located near the singularity.

As another important point, the laboratory analogues constitute nice examples for the distinction between universal (emergent) phenomena and system-specific (microscopic) features, which is also crucial for our understanding of quantum gravity. While an effective metric, i.e., an effective Lorentz invariance, seems to emerge naturally in many condensed matter systems, the principle of equivalence and the Einstein equations require some additional input (kinematic versus dynamics). The combination of kinematic and dynamics becomes relevant for the back-reaction of quantum fluctuations onto the approximately classical background. Studying Bose-Einstein condensates as an example, one finds that the naive sum of the zero-point energy/pressure of the phonon modes up to some cut-off yields a completely wrong result⁷⁰. This lesson should be relevant for the cosmological constant problem, for example.

The analogy to condensed matter does also teach us that quantizing a classical macroscopic theory is not always working (even though the quantization of the linearized quasi-particles might work). In the case of electrodynamics, the direct transition from classical to quantum description was very successful. For fluid dynamics, however, this procedure is very problematic. For example, starting from the classical Euler equation, one does not get the quantization of vorticity right. In the case of superfluids, for instance, the circulation quantum depends on the mass of the condensed particles, which does not appear at all in the classical Euler equation. The main question, then, is whether gravity is more similar

to electrodynamics (where a direct quantization works very well) or to fluid dynamics (where the correct quantization requires some knowledge about the microscopic structure). The underlying symmetries, the complex constraint structure, and the UV-divergences resulting from a naive quantization seem to point towards the latter – but this question must be answered in the future.

Finally, the analogy between condensed matter and gravity does also allow us to understand laboratory physics from a different point of view, i.e., in terms of the universal geometrical concepts (e.g., horizons) known from gravity. For low energies, we may forget the underlying microscopic structure and consider the effective metric only. As a result, very different condensed matter systems – such as an expanding fluid on the one hand and a medium at rest with a time-dependent speed of sound

on the other hand – may exhibit basically the same physical effects (e.g., cosmological particle creation) due to the coordinate invariance of the effective metric.

Acknowledgements

This work was supported by the Emmy-Noether Programme of the German Research Foundation (DFG) under grant # SCHU 1557/1. The author acknowledges fruitful discussions with Bill Unruh and many others (who cannot be listed here due to the irreconcilability of doing justice to everyone of the one hand and space restrictions on the other hand.)

-
- [1] N. D. Birrell and P. C. W. Davies, *Quantum Fields in Curved Space* (Cambridge University Press, Cambridge, England 1982); S. A. Fulling, *Aspects of Quantum Field Theory in Curved Space-Time* (Cambridge University Press, Cambridge, England 1989).
- [2] S. W. Hawking, *Black Hole Explosions*, Nature **248**, 30 (1974); *Particle Creation by Black Holes*, Commun. Math. Phys. **43**, 199 (1975).
- [3] J. D. Bekenstein, *Black Holes And The Second Law*, Lett. Nuovo Cim. **4**, 737 (1972); *Black Holes And Entropy*, Phys. Rev. D **7**, 2333 (1973); *Generalized Second Law Of Thermodynamics In Black Hole Physics*, ibid. **9**, 3292 (1974); *Statistical Black Hole Thermodynamics*, ibid. **12**, 3077 (1975); J. M. Bardeen, B. Carter and S. W. Hawking, *The Four Laws Of Black Hole Mechanics*, Commun. Math. Phys. **31**, 161 (1973).
- [4] C. Barceló, S. Liberati, and M. Visser, *Analogue Gravity*, Living Rev. Rel. **8**, 12 (2005).
- [5] G. E. Volovik, *Universe in a Helium Droplet* (Oxford University Press, Oxford, 2003).
- [6] M. Novello, M. Visser, and G. Volovik (editors), *Artificial Black Holes* (World Scientific, Singapore, 2002).
- [7] R. Schützhold and W. G. Unruh (eds.), *Quantum Analogues: From Phase Transitions to Black Holes & Cosmology*, Springer Lecture Notes in Physics **718** (2007).
- [8] R. Schützhold and M. Uhlmann, *Horizon Analogues in the Laboratory*, Proceedings of the Memorial Symposium for Gerhard Soff (April 25 and 26, 2005, Frankfurt, Germany); R. Schützhold, *Summary of session E1: analogue gravity*, Class. Quant. Grav. **25**, 114027 (2008); *Emergent Horizons in the Laboratory*, Class. Quant. Grav. **25**, 114011 (2008); *‘Exotic’ quantum effects in the laboratory?*, Phil. Trans. R. Soc. A (in press).
- [9] R. P. Kerr, *Gravitational Field Of A Spinning Mass As An Example Of Algebraically Special Metrics*, Phys. Rev. Lett. **11**, 237 (1963).
- [10] R. Penrose, *Gravitational Collapse: The Role Of General Relativity*, Riv. Nuovo Cim. **1**, 252 (1969); Gen. Rel. Grav. **34**, 1141 (2002).
- [11] W. H. Press and S. A. Teukolsky, *Floating Orbits, Superradiant Scattering and the Black-hole Bomb*, Nature **238**, 211 (1972).
- [12] Ya. B. Zel’dovich, *Generation of Waves by a Rotating Body*, JETP Lett. **14**, 180 (1971); A. A. Starobinsky, *Amplification of waves during reflection from a rotating “black hole”* Soviet Physics JETP **31**, 28 (1973).
- [13] W. G. Unruh, *Notes on Black Hole Evaporation*, Phys. Rev. D **14**, 870 (1976) J. Bisognano and E. H. Wichmann, *On the duality condition for quantum fields*, J. Math. Phys. **17**, 303 (1976).
- [14] W. Israel, *Thermo Field Dynamics of Black Holes*, Phys. Lett. A **57**, 107 (1976); Y. Takahashi and H. Umezawa, *Thermo Field Dynamics*, Collective Phenomena **2**, 55 (1975); Int. J. Mod. Phys. B **10**, 1755 (1996).
- [15] T. Jacobson, *Black Hole Evaporation and Ultrashort Distances*, Phys. Rev. D **44**, 1731 (1991).
- [16] W. G. Unruh and R. Schützhold, *On the universality of the Hawking effect*, Phys. Rev. D **71**, 024028 (2005); T. Jacobson and D. Mattingly, *Hawking radiation on a falling lattice*, ibid. **61**, 024017 (2000); S. Corley, *Computing the spectrum of black hole radiation in the presence of high frequency dispersion: An analytical approach*, ibid. **57**, 6280 (1998); R. Brout, S. Massar, R. Parentani and P. Spindel, *Hawking Radiation Without Transplanckian Frequencies*, ibid. **52**, 4559 (1995); Y. Himemoto and T. Tanaka, *Generalization of the model of Hawking radiation with modified high frequency dispersion relation*, ibid. **61**, 064004 (2000); H. Saida and M. Sakagami, *Black hole radiation with high frequency dispersion*, ibid. **61**, 084023 (2000).
- [17] R. Schützhold and W. G. Unruh, *On the origin of the particles in black hole evaporation*, arXiv:0804.1686.
- [18] D. M. Eardley, *Death of White Holes in the Early Universe*, Phys. Rev. Lett. **33**, 442 (1974).
- [19] S. Corley and T. Jacobson, *Black hole lasers*, Phys. Rev. D **59**, 124011 (1999).
- [20] G. W. Gibbons and S. W. Hawking, *Cosmological event horizons, thermodynamics, and particle creation*, Phys. Rev. D **15**, 2738 (1977).
- [21] P. A. M. Dirac, *The Quantum Theory of the Electron*, Proc. Roy. Soc. (London) A **117**, 610 (1928); *The Quantum Theory of the Electron, Part II*, ibid. **118**, 351 (1928); *A Theory of Electrons and Protons*, ibid. **126**, 360 (1930).

- [22] O. Klein, *Die Reflexion von Elektronen an einem Potentialsprung nach der relativistischen Dynamik von Dirac*, Z. Phys. **53**, 157 (1929).
- [23] F. Sauter, *Über das Verhalten eines Elektrons im homogenen elektrischen Feld nach der relativistischen Theorie Diracs*, Z. Phys. **69**, 742 (1931); *ibid.* **73**, 547 (1931).
- [24] W. Heisenberg and H. Euler, *Consequences of Dirac's Theory of Positrons*, Z. Phys. **98**, 714 (1936).
- [25] J. Schwinger, *On Gauge Invariance and Vacuum Polarization*, Phys. Rev. **82**, 664 (1951).
- [26] W. Gordon, *Zur Lichtfortpflanzung nach der Relativitätstheorie*, Ann. Phys. (Leipzig) **72** (1923) 421.
- [27] W. G. Unruh, *Experimental Black Hole Evaporation?*, Phys. Rev. Lett. **46**, 1351 (1981).
- [28] P. Painlevé, *La Mécanique classique et la théorie de la relativité*, C. R. Hebd. Seances Acad. Sci. (Paris) **173** (1921) 677; A. Gullstrand, *Allgemeine Lösung des statischen Einkörperproblems in der Einsteinschen Gravitationstheorie*, Ark. Mat. Astron. Fys. **16** (1922) 1; G. Lemaître, *L'univers en expansion*, Ann. Soc. Sci. (Bruxelles) A **53** (1933) 51.
- [29] M. I. Katsnelson, K. S. Novoselov, and A. K. Geim, *Chiral tunnelling and the Klein paradox in graphene*, Nature Physics **2**, 620 (2006).
- [30] C. Barcelo, S. Liberati and M. Visser, *Analogue gravity from field theory normal modes?*, Class. Quant. Grav. **18** (2001) 3595; *Refringence, field theory, and normal modes*, *ibid.* **19** (2002) 2961; C. Barcelo, M. Visser, and S. Liberati, *Einstein gravity as an emergent phenomenon?*, Int. J. Mod. Phys. D **10** (2001) 799.
- [31] R. Schützhold and W. G. Unruh, *Gravity wave analogues of black holes*, Phys. Rev. D **66** (2002) 044019.
- [32] R. Schützhold and W. G. Unruh, *Hawking radiation in an electro-magnetic wave-guide?*, Phys. Rev. Lett. **95**, 031301 (2005).
- [33] T. G. Philbin *et al.*, *Fiber-Optical Analog of the Event Horizon*, Science **319**, 1367 (2008).
- [34] W. G. Unruh and R. Schützhold, *On Slow Light as a Black Hole Analogue*, Phys. Rev. D **68** (2003) 024008; see also U. Leonhardt and P. Piwnicki, *Relativistic Effects of Light in Moving Media with Extremely Low Group Velocity*, Phys. Rev. Lett. **84** (2000) 822; M. Visser, *Comment on "Relativistic Effects of Light in Moving Media with Extremely Low Group Velocity"*, *ibid.* **85** (2000) 5252; U. Leonhardt and P. Piwnicki, *Reply to comment on "Relativistic Effects of Light in Moving Media with Extremely Low Group Velocity"*, *ibid.* **85** (2000) 5253.
- [35] R. Schützhold *et al.*, *Analogue of cosmological particle creation in an ion trap*, Phys. Rev. Lett. **99**, 201301 (2008).
- [36] P. M. Alsing, J. P. Dowling, and G. J. Milburn, *Ion Trap Simulations of Quantum Fields in an Expanding Universe*, Phys. Rev. Lett. **94**, 220401 (2005).
- [37] F. Dalfovo, S. Giorgini, L. P. Pitaevskii, and S. Stringari, *Theory of Bose-Einstein condensation in trapped gases*, Rev. Mod. Phys. **71**, 463 (1999); A. J. Leggett, *Bose-Einstein condensation in the alkali gases: Some fundamental concepts*, Rev. Mod. Phys. **73**, 307 (2001).
- [38] W. G. Unruh, *Measurability of Dumb Hole Radiation?*, in M. Novello, M. Visser, and G. Volovik (editors), *Artificial Black Holes* (World Scientific, Singapore, 2002).
- [39] M. Uhlmann, Y. Xu, and R. Schützhold, *Aspects of Cosmic Inflation in Expanding Bose-Einstein Condensates*, New J. Phys. **7**, 248 (2005).
- [40] P. O. Fedichev and U. R. Fischer, *"Cosmological" quasi-particle production in harmonically trapped superfluid gases*, Phys. Rev. A **69**, 033602 (2004); C. Barcelo, S. Liberati and M. Visser, *Analogue gravity from Bose-Einstein condensates*, Class. Quant. Grav. **18**, 1137 (2001).
- [41] R. Schützhold, *Dynamical zero-temperature phase transitions and cosmic inflation/deflation*, Phys. Rev. Lett. **95**, 135703 (2005).
- [42] U. R. Fischer and R. Schützhold, *Quantum simulation of cosmic inflation in two-component Bose-Einstein condensates*, Phys. Rev. A **70**, 063615 (2004).
- [43] S. Weinfurter, A. White and M. Visser, *Trans-Planckian physics and signature change events in Bose gas hydrodynamics*, Phys. Rev. D **76**, 124008 (2007).
- [44] E. A. Donley *et al.*, *Dynamics of collapsing and exploding Bose-Einstein condensates*, Nature **412**, 295 (2001); see also E. A. Calzetta and B. L. Hu, *Early Universe Quantum Processes in BEC Collapse Experiments*, Int. J. Theo. Phys. **44**, 1691 (2005); S. Wuester *et al.*, *Quantum depletion of collapsing Bose-Einstein condensates*, Phys. Rev. A **75**, 043611 (2007).
- [45] P. Jain, S. Weinfurter, M. Visser and C. W. Gardiner, *Analogue model of a FRW universe in Bose-Einstein condensates: Application of the classical field method*, Phys. Rev. A **76**, 033616 (2007).
- [46] P. O. Fedichev and U. R. Fischer, *Gibbons-Hawking Effect in the Sonic de Sitter Space-Time of an Expanding Bose-Einstein-Condensed Gas*, Phys. Rev. Lett. **91**, 240407 (2003); *Observer dependence for the phonon content of the sound field living on the effective curved space-time background of a Bose-Einstein condensate*, Phys. Rev. D **69**, 064021 (2004).
- [47] A. Retzker, J. I. Cirac, M. B. Plenio, B. Reznik, *Detection of acceleration radiation in a Bose-Einstein condensate*, arXiv:0709.2425.
- [48] H. Takeuchi, M. Tsubota and G. E. Volovik, *Zel'dovich-Starobinsky Effect in Atomic Bose-Einstein Condensates: Analogy to Kerr Black Hole*, J. Low Temp. Phys. **150**, 624 (2008).
- [49] M. Visser, and S. Weinfurter, *Massive Klein-Gordon equation from a BEC-based analogue spacetime*, Phys. Rev. D **72**, 044020 (2005).
- [50] S. Liberati, M. Visser, and S. Weinfurter, *Naturalness in emergent spacetime*, Phys. Rev. Lett. **96**, 151301 (2006).
- [51] L. J. Garay, J. R. Anglin, J. I. Cirac, and P. Zoller, *Sonic Analog of Gravitational Black Holes in Bose-Einstein Condensates*, Phys. Rev. Lett. **85**, 4643 (2000).
- [52] S. Wüster and C. M. Savage, *Limits to the analogue Hawking temperature in a Bose-Einstein condensate*, Phys. Rev. A **76**, 013608 (2007).
- [53] R. Schützhold, *On the detectability of quantum radiation in Bose-Einstein condensates*, Phys. Rev. Lett. **97**, 190405 (2006).
- [54] R. Balbinot *et al.*, *Non-local density correlations as signal of Hawking radiation in BEC acoustic black holes*, arXiv:0711.4520; I. Carusotto *et al.*, *Numerical observation of Hawking radiation from acoustic black holes in atomic BECs*, arXiv:0803.0507.
- [55] J. Dziarmaga and K. Sacha, *Bose-Einstein-condensate heating by atomic losses*, Phys. Rev. A **68**, 043607 (2003).
- [56] S. Wuester, *Phonon background versus analogue Hawking radiation in Bose-Einstein condensates*,

arXiv:0805.1358.

- [57] G. E. Volovik, *The hydraulic jump as a white hole*, Pisma Zh. Eksp. Teor. Fiz. **82** 706 (2005); JETP Lett. **82** 624 (2005).
- [58] G. Rousseaux *et al.*, *Observation of negative-frequency waves in a water tank: A classical analogue to the Hawking effect?* New J. Phys. **10**, 053015 (2008).
- [59] R. Schützhold, G. Plunien, and G. Soff, *Dielectric black hole analogs*, Phys. Rev. Lett. **88** (2002) 061101.
- [60] T. Tajima and G. Mourou, *Zettawatt-exawatt lasers and their applications in ultrastrong-field physics*, Phys. Rev. ST Accel. Beams **5**, 031301 (2002).
- [61] P. Chen and T. Tajima, *Testing Unruh radiation with ultra-intense lasers*, Phys. Rev. Lett. **83**, 256 (1999).
- [62] W. G. Unruh and R. M. Wald, *What Happens When An Accelerating Observer Detects A Rindler Particle*, Phys. Rev. D **29**, 1047 (1984).
- [63] R. Schützhold, G. Schaller, and D. Habs, *Table-top creation of entangled multi-keV photon pairs via the Unruh effect*, Phys. Rev. Lett. **100**, 091301 (2008); *Signatures of the Unruh effect from electrons accelerated by ultra-strong laser fields*, *ibid.* **97**, 121302 (2006).
- [64] H. C. Rosu, *Hawking-like and Unruh like effects: Toward experiments?*, Grav. Cosmol. **7**, 1 (2001); *On the estimates to Measure Hawking Effect and Unruh Effect in the Laboratory*, Int. J. Mod. Phys. D **3**, 545 (1994).
- [65] J. S. Bell and J. M. Leinaas, *The Unruh Effect And Quantum Fluctuations Of Electrons In Storage Rings*, Nucl. Phys. B **284**, 488 (1987); W. G. Unruh, *Acceleration radiation for orbiting electrons*, Phys. Rept. **307**, 163 (1998).
- [66] M. O. Scully *et al.*, *Enhancing Acceleration Radiation from Ground-State Atoms via Cavity Quantum Electrodynamics*, Phys. Rev. Lett. **91**, 243004 (2003); see also B. L. Hu and A. Roura, *Comment on “Enhancing Acceleration Radiation from Ground-State Atoms via Cavity Quantum Electrodynamics”*, *ibid.* **93**, 129301 (2004); M. O. Scully *et al.*, *Reply to Comment on “Enhancing Acceleration Radiation from Ground-State Atoms via Cavity Quantum Electrodynamics”*, *ibid.* **93**, 129302 (2004); and A. Belyanin *et al.*, *Quantum electrodynamics of accelerated atoms in free space and in cavities*, Phys. Rev. A **74**, 023807 (2006).
- [67] <http://www.extreme-light-infrastructure.eu/>
- [68] S. Gordienko, A. Pukhov, O. Shorokhov, and T. Baeva, *Relativistic Doppler Effect: Universal Spectra and Zep-tosecond Pulses*, Phys. Rev. Lett. **93**, 115002 (2004); *Coherent Focusing of High Harmonics: A New Way Towards the Extreme Intensities*, Phys. Rev. Lett. **94**, 103903 (2005); S. V. Bulanov, T. Esirkepov, and T. Tajima, *T. Light Intensification towards the Schwinger Limit*, Phys. Rev. Lett. **91**, 085001 (2003).
- [69] R. Schützhold, H. Gies, and G. Dunne, *Dynamically assisted Schwinger mechanism*, to appear soon.
- [70] Ralf Schützhold, *Quantum back-reaction problems*, Proceedings of Science (QG-Ph) 036 (2007); R. Schützhold, M. Uhlmann, Y. Xu, and U. R. Fischer, *Quantum back-reaction in dilute Bose-Einstein condensates*, Phys. Rev. D **72**, 105005 (2005).